Clays and Clay Minerals, Vol. 62, No. 3, 211–223, 2014.

THE SURFACE MODIFICATION OF ZEOLITE 4A AND ITS EFFECT ON THE WATER-ABSORPTION CAPABILITY OF STARCH-G-POLY (ACRYLIC ACID) COMPOSITE

ZHANG YAN[1,3], ZHAO LIN[1,2,*], MA KAI[2], AND MAO GUOZHU[2]

[1] School of Chemical Engineering and Technology, Tianjin University, 92 Weijin Road, Nankai District, Tianjin 300072, P.R. China
[2] School of Environment Science and Engineering, Tianjin University, 92 Weijin Road, Nankai District, Tianjin 300072, P.R. China
[3] School of Chemistry and Chemical Engineering, Yulin university, 4 Chongwen Road, Yulin City , Shaanxi 719000, P.R. China

Abstract—The surface modification of Zeolite 4A using cetyl trimethyl ammonium bromide (CTAB) as a modifier *via* an ultrasonic method was carried out and the surface physicochemical properties measured. Response surface methodology (RSM) was developed with CTAB concentration, handling time, and handling temperature as variables, to help predict the performance of the modified zeolite under particular conditions. The influence of organic-modified surface treatment and of the amount of modified zeolite on the water-absorption capability of starch-g-poly (acrylic acid) hydrogel composites was also assessed. The results showed that the channels and skeleton structure of zeolite 4A were unchanged after organic modification by CTAB and the surface modification was effective. The results suggest that organic-modified zeolite 4A has improved the water-absorption capability.

Key Words—Organic Modification, Response Surface Methodology, Superabsorbent Composite, Water Absorption, Zeolite 4A.

INTRODUCTION

Superabsorbents have a three-dimensional network of hydrophilic polymers that can swell to an equilibrium state, and retain a significant amount of water and/or biological fluids. Because of this property, superabsorbents have been used extensively in areas such as sanitary goods, waste-water treatment, agriculture, and in medicine for drug-delivery systems since the first superabsorbent polymer was reported by the U.S. Department of Agriculture in 1976 (Li and Wang, 2005; Mohana Raju and Padmanabha Raju, 2001; Lokhande and Gotmare, 1999; Weaver *et al.*, 1976). The absorption capacity is dominated by the ability of three-dimensional networks of superabsorbents to absorb free water. The water-absorption capacity of a superabsorbent is determined both by extension, caused by ionic-charge repulsion of the macromolecular electrolyte, and by expansion resistance, caused by the cross-linking structure and hydrogen bonding (Zhou *et al.*, 2012). The internal micromorphology of a superabsorbent polymer (SAP) also affects directly its absorption mechanism and characteristics (Wang and Zhang, 2006). Most superabsorbents are based on poly(acrylic acid), however, which has poor biodegradability in soil, for example, and so poses an environmental problem. The increasing prices of petrochemical feedstock, concern about waste disposal, and the desire to use renewable and environmentally friendly resources have prompted recent research interest in this area. Starch-grafted copolymers have received considerable attention because the introduction of this biodegradable and low-priced natural starch not only improves the biodegradability of the corresponding superabsorbents, but also reduces dependence on petrochemical monomers (Lanthong *et al.*, 2006; Zdanowicz *et al.*, 2010). Traditional superabsorbent networks of synthetic polymers often have limitations other than poor biodegradability which restrict their application. Many methods have been applied to improve the absorption properties and to extend the range of possible applications of SAPs (Lee and Yang, 2004). Inorganic-organic superabsorbent composites based on mica, attapulgite, and kaolinite have been created in attempts to realize smaller production costs and better water-absorption capacity (Zhang *et al.*, 2006). Starch-grafted acrylic acid/clinoptilolite/fly-ash composite with a water-absorption capacity of 320 g/g was prepared by Zhang *et al.* (2011) who deemed it unsatisfactory. Introduction of the fly-ash modified the zeolite network resulting in its local dissolution and stimulated aggregation that decreased the water absorbency of the composites.

Studies of composites based on zeolites were suggested. Zeolites are highly crystalline aluminosilicates represented by the general formula $M^{+}_{x/n}[(AlO_2)_x(SiO_2)_y]^{x-}\cdot ZH_2O$ (where M is a metal cation, a proton, or less frequently, a charged molecule) (Rožić and Miljanić, 2011). Zeolite crystals are characterized by a regular three-dimensional network of intracrystalline nanovoids. Zeolites have been applied in various fields as sorbents (Faghihian *et al.*, 2013; Rožić and Miljanić, 2011; Haggerty and Bowman, 1994), soil amendments

* E-mail address of corresponding author:
zhaolin@tju.edu.cn
DOI: 10.1346/CCMN.2014.0620305

(Bernardi *et al.*, 2013; Zwingmann *et al.*, 2011), ion exchangers (Wang *et al.*, 2011, 2012; Stojakovic *et al.*, 2011), and catalysts (Saxena *et al.*, 2013) and are classified into various types according to their structures, *e.g.* A, X, Y, ZSM-5, and clinoptilolite. Among them, single-phase zeolite 4A has been of great interest because of its large cation exchange capacity and its large number of acid sites due to its 8-ring, 6-ring, and 4-ring channel structure with the largest cavity dimension measuring 0.41 nm × 0.41 nm; because of this, zeolite 4A is used widely in ion-exchange processes (Hui *et al.*, 2005). Zeolite 4A also has significant absorption capacity, large cation-exchange capacity, and excellent water-holding capacity in the free channels, leading to the interesting and potentially important application of zeolite 4A as a soil amendment in agriculture. The addition of synthetic zeolite pellets to soils contaminated with cadmium was reported by Gworek (1992) to reduce significantly the concentrations of Cd in the roots and shoots of a range of crop plants. Use of synthetic zeolite type 4A, at application rates of 1% by soil weight, caused reductions in Cd concentrations of up to 86% in leaves of lettuce grown in pots, compared to controls with no added zeolites. Asb-A zeolites were synthesized by Le Van Mao *et al*. (1991) who found that these zeolites helped soil to retain moisture for extended periods of time. When the amount of the zeolite material added was 5 wt.% the length of time for which moisture was retained was increased from 3 h to 7 days. The water-retention capacity is heavily dependent on the textural properties of the zeolite materials and the zeolite materials exhibited no *in vitro* cell toxicity. To date, no research has been published on the water-absorption ability of superabsorbent composites in relation to zeolite 4A.

Micro-sized zeolite 4A particles show a strong tendency to aggregate due to their specific surface structure and surface interactions resulting in irregular dispersal in polymeric systems when added directly without pretreatment. The apparent difference between the interfacial characteristics of zeolite 4A and the polymer matrix has resulted in poor compatibility during polymeric synthesis (Guo *et al*., 1999; Ahmad and Hägg, 2003; Khoonsap and Amnuaypanich, 2011). These drawbacks decrease the final absorption capacity of the composite. Chemical modification of zeolite 4A before it is polymerized removes these problems. Surfactants are water-soluble organic molecules which have hydrophilic and hydrophobic properties. Cationic surfactants with positively charged head groups attached to hydrocarbon moieties, such as alkyl ammonium compounds, have been utilized to form organically modified clays (Irani *et al.*, 2013).

The optimization technique referred to as 'one-variable-at-a-time' is often applied to determine the effects of the relevant parameters in the modification process (Wang, *et al*., 2006). The major disadvantage is that it does not account for the interactive effects among the variables studied and so does not illustrate all the effects of the parameter on the response (Lundstedt *et al.*, 1998). Another disadvantage of the one-factor optimization is the increase in the number of experiments required to conduct the research, which leads to increased time and expense as well as increased consumption of reagents and materials. To overcome these problems, response surface methodology (RSM), one of the most sophisticated multivariate statistical methods used in analytical optimization, was deployed. Response surface methodology is a collection of mathematical and statistical techniques based on the fit of a polynomial equation to the experimental data which must describe the behavior of a set of data with the objective of making statistical predictions (Bezerra *et al.*, 2008). The method is used under experimental conditions where a response or a set of responses of interest are influenced by several variables; the levels of these variables can be optimized simultaneously to reach optimal system performance using minimum experimental effort. Box-Behnken designs (BBD) are a class of rotatable or nearly rotatable second-order designs based on three-level incomplete designs. In the present study, a BBD design was proposed to fit a second-order model for optimal conditions studies (Ferreira *et al.*, 2007).

In the present study, organically modified zeolite 4A was synthesized under ultrasonic waves using CTAB as a surfactant to improve the surface properties of zeolite 4A with the aim of increasing its surface reactivity to the starch-g-poly (acrylic acid) matrix. The RSM was applied to determine the optimum modification conditions of the organic-modified zeolite 4A. In addition, the effects of surface treatment of zeolite 4A and the water-absorption capacity of starch-g-poly(acrylic acid)/organic-modified 4A composite were also investigated.

EXPERIMENTAL

Materials

Zeolite 4A purchased from Nan Kai University Catalyst Co., Ltd. (Tianjin, China) was milled using an agate mortar to pass through a 320-mesh screen and treated with NaOH for 24 h followed by washing with distilled water and then dried at 100ºC for 12 h. Zeolite 4A CTAB with a molar mass of 364.46 g/mol and a minimum of 99% of active substance was used. Corn starch was supplied by Tianjin Dingyan Trading & Property Co., Ltd. (Tianjin. China). Acrylic acid was supplied by Tianjin Damao Chemical Reagent Factory (Tianjin, China) and purified by recrystallization. Potassium persulfate was purchased from Tianjin Kewei Chemical Reagent Factory (Tianjin, China) and recrystallized before use. N,N-methylenebisacrylamide (MBA) was supplied by Tianjin Kemiou Chemical Reagent Corp. (Tianjin, China). All the other chemicals were of analytical grade and used without further purification.

https://doi.org/10.1346/CCMN.2014.0620305 Published online by Cambridge University Press

Synthesis of modified zeolite 4A

A 3-factors-3-level response surface Box-Behnken design, which required 17 runs including three replicates of the central run, was used in the modification of zeolite 4A with CTAB as the organic modifier under ultrasonic waves. The factors were: CTAB concentration (X_1 = 43.1, 59.1, and 75.1 mmol/L), ultrasonic handling time (X_2 = 30, 60, and 90 min), and handling temperature (X_3 = 30, 50, and 70ºC). Second-order polynomial regression models, as shown below (equation 1) were fitted to the response, in terms of the factors selected:

$$Y_i = b_o + \Sigma b_i X_i + \Sigma b_{ii} X_i^2 + \Sigma\Sigma b_{ij} X_i X_j + \varepsilon \quad (1)$$

Where Y_i represents the response; b_o, b_i, b_{ii}, and b_{ij} were the regression coefficients, X values were the independent factors and ε was the experimental error. Only significant coefficients ($r \leqslant 0.005$) and corresponding terms were included in the model. The factors were coded in three levels (−1, 0, and 1) before fitting the model.

Five grams (5 g) of zeolite 4A and the specified aqueous solution of CTAB were placed in a 500 mL conical flask. The flask was kept in a water bath at the required temperature (30, 50, 70ºC) under ultrasonic waves for specified periods of time (30, 60, 90 min). The reaction product was filtered and washed with aqueous ethanol several times to ensure the complete removal of the Br^-. The product was washed with distilled water and dried at 60ºC, then milled to pass a 180 mesh sieve after grinding using an agate mortar.

Zeolite 4A has the ability to attract positively charged ions due to its electrically neutral framework. The basic structure of zeolite is the Si−O (SiO_4) tetrahedron. During the course of modification with CTAB, Al^{3+} replaces Si^{4+}, so that the entire Al−O tetrahedron bears a single negative charge. In order to maintain electrical neutrality, appropriate positively charged cations must be introduced to offset the negative charge around the vicinity of the Al−O tetrahedron. Sodium or potassium ions are adsorbed on external surfaces and in the pores to balance the charge.

The CTAB as cationic surfactant can diffuse on the external surface and replace the adsorbed ions. When CTAB replaces the adsorbed ions the surfactant acts further to change the charge and chemistry of the zeolite 4A surface. The surfactant adsorbs with its positively charged head group ($C_{16}H_{33}(CH_3)_3N^+$ ions) next to the negatively charged zeolite surface, forcing the hydrophobic surfactant tail to adsorb and be exposed to the solution. Thus, while the native zeolite surface is hydrophilic, the adsorption of a small amount of surfactant on the surface can render it hydrophobic. As shown in equation 2:

$$C_{16}H_{33}(CH_3)_3N^+Br + M\text{-Zeolite 4A} \rightarrow C_{16}H_{33}(CH_3)_3N^+\text{-Zeolite} + MBr \quad (2)$$

(where $M = Na^+$, Ca^{2+}, Mg^{2+}).

Determination of results of modification

Stability of zeolite 4A in deionized water. Modified zeolite 4A (5 g) under optimum conditions with CTAB was added to 400 mL of distilled water using a 500 mL Schott Duran Separating Funnel (Zhou *et al.*, 2005) under stirring to obtain suspension. The system was left to stand for 30 min until no modified zeolite 4A was seen to fall to the bottom of funnel. A test without CTAB was done under the same conditions.

Active index. Zeolite 4A is wetted easily in distilled water due to its hydrophilic surface. Through organic modification, its hydrophilic surface will change to hydrophobic as a result of which organic-modified zeolite 4A will float on the surface of the distilled water instead of being wetted. This makes it easy to test for the modification. 'Active index' is a special term introduced here which means the ratio of the weight of the floating organic-modified zeolite 4A to the total weight of organic-modified zeolite 4A, to explain the effect of the modification reaction. The exact weights of the two kinds of organic-modified zeolite 4A are the values needed to determine the active index.

Stability of zeolite 4A in deionized water. The modified zeolites 4A were divided into two types: one was sediment deposited at the bottom of the vessel, the other was that found floating on the surface of the distilled water. Both types were filtered, dried, and weighed. The active index was calculated from equation 3:

$$H = \left(\frac{M_1}{M}\right) \times 100\% \quad (3)$$

where H denotes the 'active index' of the modified zeolite 4A (%); M denotes weights of total modified zeolite 4A (g), and M_1 denotes sediments from modified zeolite 4A (g). The blank test without CTAB was done under the same conditions as above. All procedures were carried out in triplicate (n = 3) and the value is the mean of three replicates.

Synthesis of starch-g-poly (acrylic acid)/organic-modified zeolite 4A superabsorbent composite

The composite based on corn starch, acrylic acid, NaOH solution, and modified zeolite 4A was synthesized according to the following procedure: 4 g of corn starch was solubilized in 100 mL of distilled water at 90ºC for 60 min using a 500 mL four-neck flask equipped with a reflux condenser, a funnel, and a $N_{2(g)}$ line. Then, while the temperature was cooled to 45ºC, 5 g/L of potassium persulfate was added to the system. After 15 min, the mixed solution of sodium acrylate (acrylic acid partially neutralized with 80 mol.% NaOH solution), 5 g/L of N, N-methylenebisacrylamide (MBA), and specific amounts of modified zeolites 4A under optimum conditions (weight ratios of modified

https://doi.org/10.1346/CCMN.2014.0620305 Published online by Cambridge University Press

zeolites 4A/acrylic acid of 5−40 wt.%) were added. The water bath was heated slowly to 70ºC and kept at that temperature for 3 h to complete the polymerization reaction. Throughout the process the system was under a N_2 atmosphere. The material obtained was washed several times with ethanol to ensure the complete removal of the homopolymer. The superabsorbent was oven-dried at 75ºC. As mentioned above, a blank sample, without organic-modified zeolite 4A, was also synthesized and is referred to here as starch-g-poly (acrylic acid). A proposed mechanistic pathway for the synthesis of the starch-g-poly (acrylic acid) is presented in Figure 1 (Spagnol *et al.*, 2012).

Evaluation of water absorption for the composite

The water-absorption capacity of the composite was determined at ambient temperatures using the procedure of Alummoottil *et al.* (2010). The composite (0.1 g) was immersed in distilled water (200 mL) for 24 h to reach its swelling equilibrium (resulting from the absorption of water within the network of the composites). Residual water was removed by filtration over an 80-mesh screen for 25 min. The water-absorption capacity was calculated as the weight of the water absorbed per gram of dry composite. In addition, the sample was weighed at various time intervals to follow the kinetics of swelling in water. The water absorption for starch-g-poly (acrylic acid)/organic-modified zeolite 4A composite was determined according to equation 4:

$$W = [m/m_0] - 1 \quad (4)$$

where W was the mass of the water gained per gram of the dry composite (g/g), m was the mass of the swollen absorbent (g), and m_0 was the mass (g) of the dry composite. Three replicates were tested for each component.

X-ray diffraction analysis

The powder X-ray diffraction (XRD) traces of the samples were obtained using a Bruker X-ray diffractometer (Model D8 Advance, Bruker AXS, Madison, Wisconsin, USA) with CuKα radiation (λ = 0.15406 nm) source.

Infrared spectroscopy

Infrared spectra of unmodified zeolite 4A and the modified zeolite 4A were recorded using a Nicolet-6770 Fourier Transform Infrared (FTIR) instrument with the KBr pressed-disk technique. Spectra were taken over the spectral range 4000−400 cm^{-1} with a resolution of 4 cm^{-1}.

Scanning electron microscopy

A Nanosem 430 scanning electron microscope (SEM) with energy dispersive X-ray spectrometer (EDS) was

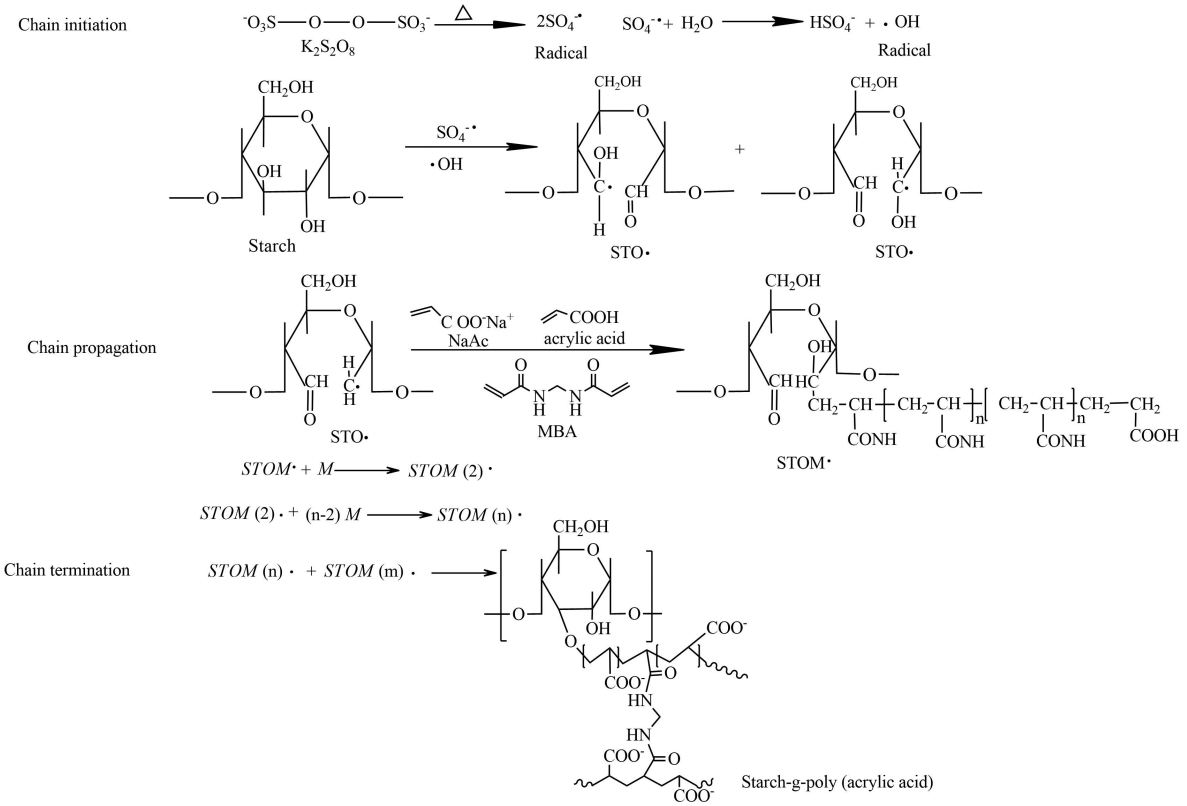

Figure 1. Proposed mechanistic pathway for synthesis of the starch-g-poly (acrylic acid).

https://doi.org/10.1346/CCMN.2014.0620305 Published online by Cambridge University Press

used to obtain secondary electron images of the unmodified zeolite 4A, modified zeolite 4A surface, starch-g-poly (acrylic acid), starch-g-poly(acrylic acid)/zeolite 4A, and starch-g-poly(acrylic acid)/organic-modified zeolite 4A. Specimens for examination by SEM were prepared by coating with a thin gold layer to enhance the conductivity and secondary electron emission characteristics and to avoid surface charging under the electron beam.

Statistical analysis

The data were analyzed statistically using the *Design-Expert* package (Razali *et al.*, 2012) to perform ANOVA (analysis of variance), to fit the second-order polynomial equations and to generate second-order surface plots (Dawood and Li, 2013). Coefficients of determination (R^2) were computed and the adequacy of the model was tested by separating the residual sum of squares into pure error and lack of fit. Three replicates were tested for each.

RESULTS AND DISCUSSION

Analysis of the stability of zeolite 4A in deionized water

Prior to modification (Figure 2a), some of the zeolite 4A dispersed into the deionized water and a large of proportion was deposited at the bottom of the Schott Duran Separating Funnel. No zeolite 4A was observed on the surface of the deionized water, demonstrating that zeolite 4A was hydrophilic. After modification under optimum conditions (Figure 2b), zeolite 4A was seen to float on the surface of the deionized water and an obvious interface layer was formed. These results revealed that CTAB was effective at modifying zeolite 4A; the dispersion of zeolite 4A in deionized water was reduced. This result is attributed to the fact that CTAB is a long-chain cationic surfactant which possesses a permanent positive charge. When brought into contact with zeolite 4A, the HDTMA exchanges selectively with the inorganic cations on the external surfaces of the zeolite and forms a surfactant layer with anion-exchange properties (Misaelides, 2011). The surfactant layer helps to improve the hydrophobic capability.

Optimization of the modification conditions for the active index

The active indexes of the samples obtained under different conditions are presented in Table 1. The active indexes of the samples ranged from 20.55 to 98.81% with the largest value obtained from the sample which was modified under the following conditions: CTAB concentration of 59.1 mmol/L, ultrasonic handling time of 60 min, and ultrasonic handling temperature of 50ºC.

Response surface methodology applied to the variables indicated that the experimental data had an

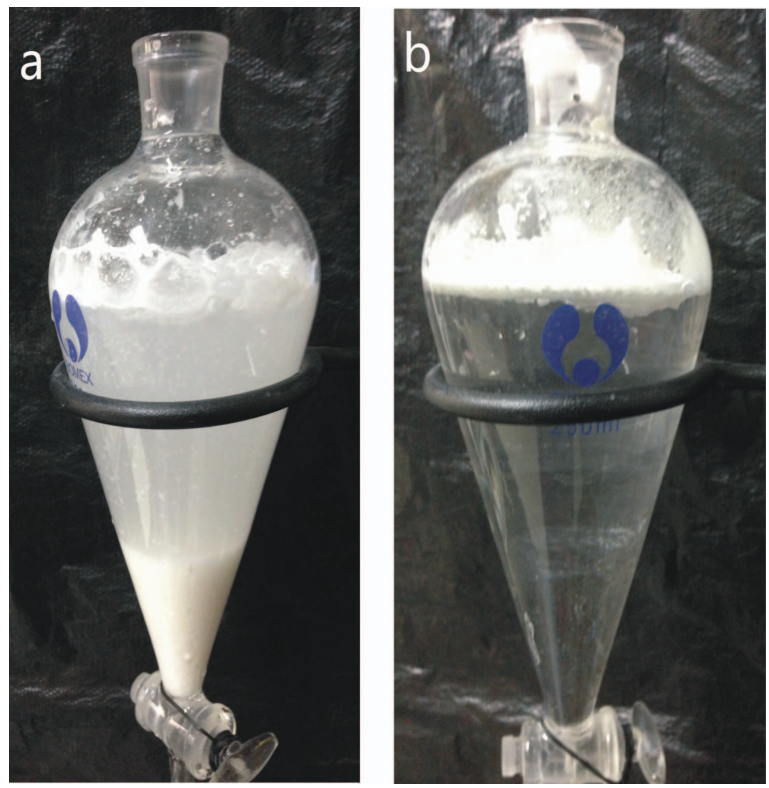

Figure 2. Stability of zeolite 4A in distilled water (a) without modification, and (b) following modification using CTAB.

https://doi.org/10.1346/CCMN.2014.0620305 Published online by Cambridge University Press

Table 1. The active index, concentration of CTAB, handling time, and handling temperature of modified zeolite 4A*.

Sample	Concentration of CTAB (mmol/L)	Handling time (min)	Handling temperature (ºC)	Active index (%)
S_1	59.1	30	50	62.96
S_2	59.1	60	50	95.26
S_3	43.1	60	70	64.05
S_4	43.1	30	50	60
S_5	75.1	60	30	97.92
S_6	43.1	90	50	88.99
S_7	59.1	60	50	97.85
S_8	75.1	30	50	22.73
S_9	59.1	60	50	98.81
S_{10}	59.1	30	30	20.55
S_{11}	59.1	90	30	84.16
S_{12}	59.1	90	70	51.93
S_{13}	59.1	60	50	99.9
S_{14}	75.1	90	50	20.13
S_{15}	75.1	60	70	34.73
S_{16}	59.1	60	50	98.19
S_{17}	43.1	60	30	55.68
Unmodified zeolite 4A*				20.48

* Values are the mean of three replicates.

adequate fit to a second-order polynomical model ($\rho < 0.5$). The model showed the active index to be a function of the reaction variable, as represented in equation 5. Only significant effects were retained in the fitted model.

$$Y = 98 - 11.65X_1 + 9.87X_2 - 5.58X_3 - 20.92X_1^2 - 29.12X_2^2 - 13.98X_3^2 - 7.90X_1X_2 - 17.89X_1X_3 - 148.66X_2X_3 \quad (5)$$

The linear and quadratic terms of the three variables have significant effects on the active index ($\rho < 0.5$). The negative coefficients of the quadratic effects of concentration of CTAB, handling time, and handling temperature indicate a decrease in the active index after reaching an optimum. The results showed that the interaction effect of concentration of CTAB and ultrasonic handling time had a significant effect on the active index ($\rho < 0.5$).

The trend was visualized in the three-dimensional surface plots of the predicted models for the active index according to changes in concentration of CTAB and handling time (Figure 3a), the CTAB concentration and the handling temperature (Figure 3b), and handling time and handling temperature (Figure 3c) on the activation of the modified zeolites 4A, when the other variable was fixed at the middle of its three given values.

The value of the coefficient of determination (R^2) was calculated as 0.83 for equation 5. The equation explains 83% of the total variation for H%, which shows the good prediction performance of the proposed model. This also confirmed that the process parameters selected had an influence on the degree of modification.

The optimum conditions for obtaining the maximum active index were predicted using the quadratic model proposed by the RSM modeling of the reaction. The values of the three factors involved were as follows: concentration of CTAB = 59.1 mmol/L, handling time = 60 min, and handling temperature = 50ºC. The active indexes of experiment and analysis under the optimum conditions mentioned above were 98.10% and 98.19%, respectively. This result verified the feasibility and effectiveness of the RSM.

XRD analysis

The diffraction patterns (Figure 4a,b) showed that both the modified and unmodified zeolite 4A presented diffraction peaks at 7.5º2θ, 16.2º2θ, 21.7º2θ, and 24.2º2θ characteristic of the 100, 110, 111, and 210 planes which are characteristic of the crystalline form of zeolite 4A. In addition, no diffraction peaks belonging to CTAB in the diffraction profile of modified zeolite 4A (Figure 4a) were found, indicating that introduction of CTAB did not lead to destruction of the zeolite 4A crystals and confirmed that the modification process took place on the surface of the zeolite 4A. The zeolite 4A cavity dimensions (0.4 nm) are much smaller than the length of the HDTMA alkyl chains (2.3 nm), and this prevents penetration by organocations into these pores. As a result, the structure of the modified zeolite 4A will not be changed during modification.

The process performed to obtain the organic-modified zeolite 4A led to XRD patterns which are characteristic of zeolite 4A with a series of sharp reflections compared to unmodified zeolite 4A. This is due to the preference of CTAB for attacking the amorphous regions of zeolite 4A under suitable temperatures through ultrasonic treatment, which increased the amount of crystalline domains in the zeolite 4A nanocrystals obtained and formed significant long-range order characteristics of the crystals.

https://doi.org/10.1346/CCMN.2014.0620305 Published online by Cambridge University Press

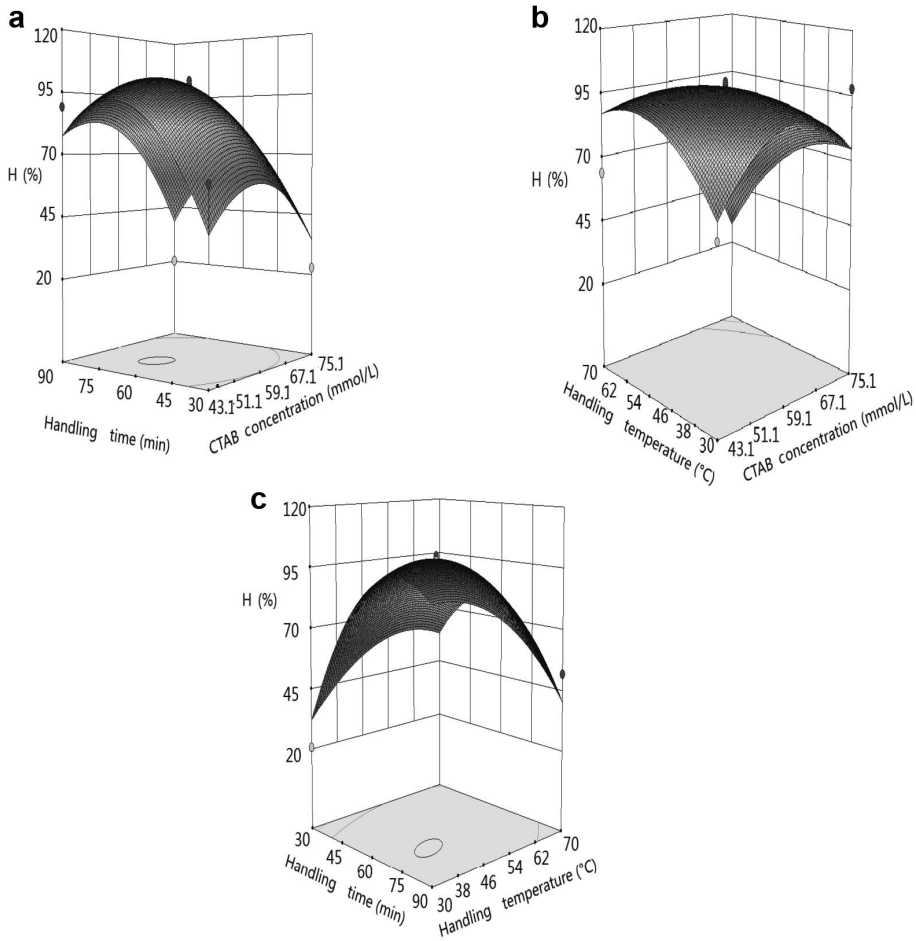

Figure 3. Response surface plots showing the effect of: (a) handling time and concentration of CTAB (X_3 = 50ºC); (b) handling temperature and concentration of CTAB (X_2 = 60 min); and (c) handling time and handling temperature (X_1 = 59.1 mmol/L) on the active index of organic-modified zeolite 4A.

FTIR analysis

The FTIR spectra of natural zeolite 4A and modified zeolite 4A under optimum conditions (Figure 5a,b) presented similar FTIR spectra in the range 500−1300 cm^{-1}. These bands are associated with Si−O−Si and Si−O−Al bending and stretching belonging to the major bands of the aluminosilicate and forming the crystal structure. At the same time, the spectra of modified zeolite 4A (Figure 5b) showed that the CTAB did not affect the linkage of Si−O and Al−O bonds. Thus, the band positions remained the same.

Two other groups of bands belonging to the modified zeolite 4A (Figure 5b) at 1630−1650 and 3500 cm^{-1} were also observed. In the first group, the absorption band is related to the bending vibration of water molecules absorbed on the natural zeolite and on the modified zeolite. In the second group, the broad band was related to the overlapping asymmetric and symmetric bands due to OH-stretching vibrations of the structural OH groups at 3433 cm^{-1}. The most intense absorption bands at 2970 and 2877 cm^{-1} arise from CH_2 asymmetric and symmetric stretching vibration modes of methylene groups in the FTIR spectrum of the crystalline CTAB. Such absorption bands can be observed in the FTIR spectrum of modified zeolite 4A (Figure 5b). For the zeolite 4A modified with CTAB, the ν_{as}, ν_s of CH_2 and methylene modes present at 1472 cm^{-1} were visible, verifying that CTAB was absorbed onto the zeolite surface and the characteristic absorption bands of zeolite 4A did not change after modification. These results were consistent with the XRD analysis.

SEM analysis

The morphology and size of the zeolite are of tremendous importance for their performance in any specific application. The SEM images of the unmodified zeolite 4A and modified zeolite 4A crystals (Figure 6) revealed shapes and sizes of zeolite 4A. The average crystal size was ~2−4 μm. The SEM observations (Figure 6a,b) confirmed the crystalline nature of zeolite 4A and the crystal morphology which can be described in terms of closely bound aggregates of small cubic

https://doi.org/10.1346/CCMN.2014.0620305 Published online by Cambridge University Press

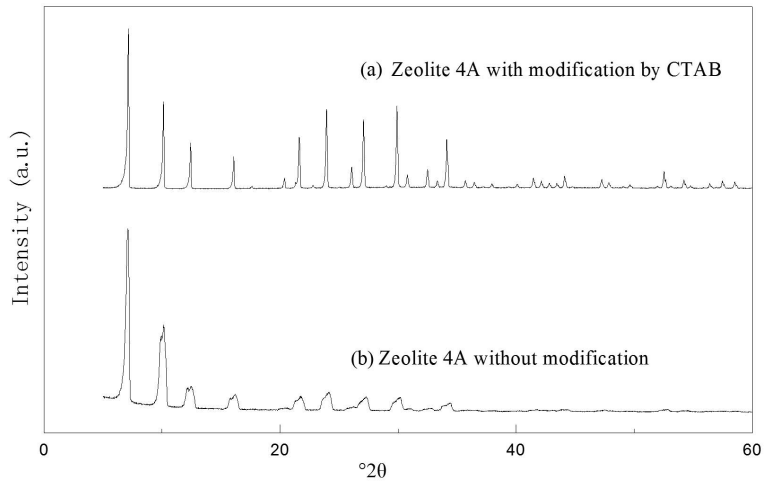

Figure 4. XRD patterns of (a) zeolite 4A following modification by CTAB under optimum conditions, and (b) zeolite 4A without modification.

particles. These crystalline aggregates, however, were not clearly visible on the SEM images of the modified zeolite 4A (Figure 6c,d). The particles of modified zeolite 4A can be dispersed favorably due to CTAB coverage on the external crystal surface and the SEM images proved that the surface modification had no obvious influence on the crystal structure of zeolite 4A.

Effect of organic-modified zeolite 4A content on water absorption by superabsorbent composites

The effect on water absorption of the amount of organic-modified zeolite 4A in the superabsorbent composite is illustrated in Figure 7. According to the results, water absorption by the superabsorbent composite increased with increasing organic-modified zeolite 4A content when the amount of organic-modified zeolite 4A was <10 wt.%. This is attributed to the fact that the presence of the organic-modified zeolite 4A in the starch-g-poly (acrylic acid) polymeric network improved the polymeric network – the long alkyl chains from CTAB are attached to the surface of the zeolite 4A rather like tadpoles, resulting in the formation of tiny hydrophobic regions in the polymeric network. The long alkyl chains are in the polymeric network when the superabsorbent composite is in a dry state; they are unfolded owing to the repulsion among the hydrophobic long alkyl chains when the superabsorbent composite is swollen in water. On the other hand, the water-absorption capacity decreased when the amount of organic-modified zeolite 4A was >10 wt.%. The excess organic-modified zeolite 4A in the superabsorbent network prevents water from being absorbed.

The surface of organic-modified zeolite 4A with long alkyl chains acts as a set of additional network points, which can participate in the polymerization reaction and

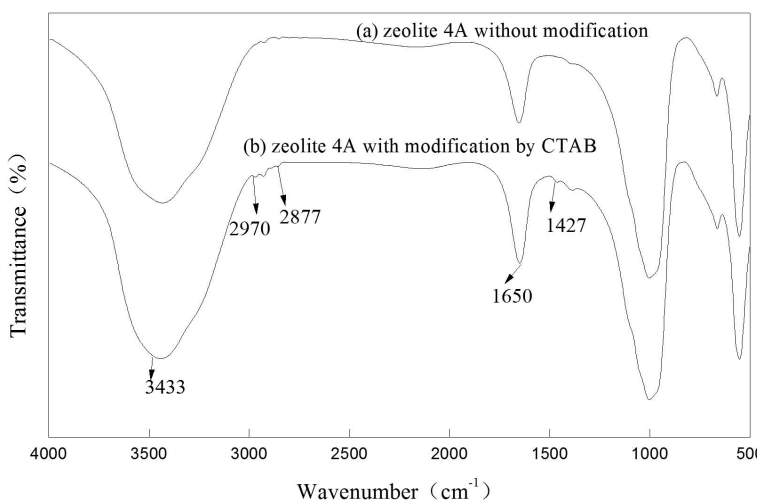

Figure 5. FTIR spectra of (a) zeolite 4A before modification, and (b) zeolite 4A following modification using CTAB under optimum conditions.

https://doi.org/10.1346/CCMN.2014.0620305 Published online by Cambridge University Press

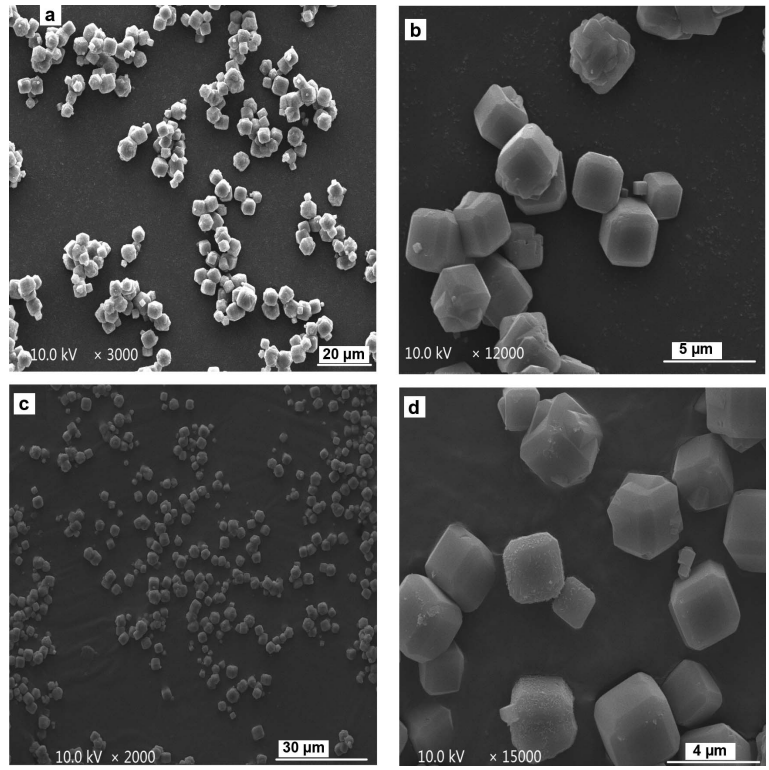

Figure 6. SEM images, at different magnifications, of (a, b) zeolite 4A without modification, and (c, d) zeolite 4A following modification using CTAB under optimum conditions.

in the formation of a 3D polymer network. As a result, the intertwining of polymerization chains was precluded and the hydrogen-bonding interactions among the hydrophilic groups, such as −COOH, −COO−, and −OH, among others, became weaker. Thus, the degree of physical crosslinking decreased and the network sites for uptake of water molecules were more available, which favors water absorption. A larger amount of organic-modified zeolite 4A, however, results in the generation of more crosslink points and fewer network

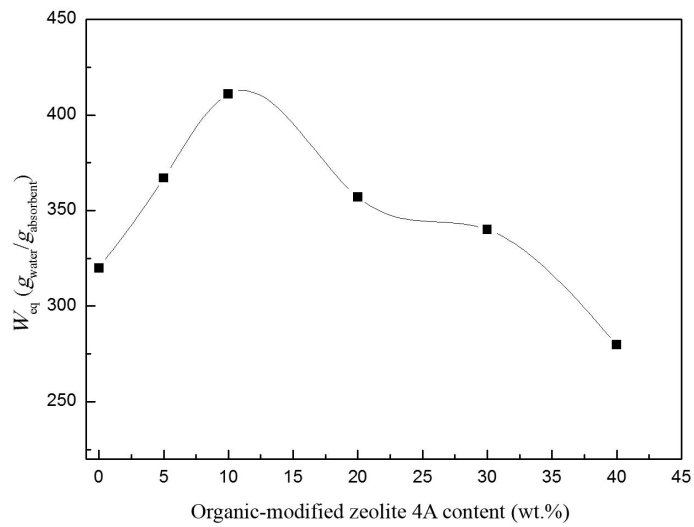

Figure 7. Effect of the amount of organic-modified zeolite 4A on water absorption by starch-g-poly (acrylic acid)/organic-modified zeolite 4A superabsorbent composite (organic-modified zeolite 4A under optimum modification conditions; concentration of potassium persulfate = 5 g/L; concentration of MBA = 5 g/L; reaction temperature = 70ºC; reaction time = 3 h; degree of neutralization = 80%).

https://doi.org/10.1346/CCMN.2014.0620305 Published online by Cambridge University Press

voids which are responsible for absorbing and taking up water molecules. Also, the excess organic-modified zeolite 4A may stack physically within the network voids. The larger the amount of organic-modified zeolite 4A, the larger is the crosslink density of the superabsorbent composite. This means that the space network for water molecules to enter becomes smaller and the water-absorption capacity decreases gradually. Some voids were plugged and so water absorption decreased for that reason also.

The water-absorption capacity of the starch-graft poly (acrylic acid) was 320 g/g. The starch-graft poly (acrylic acid)/organic-modified zeolite 4A obtained had a water-absorption capacity of 410 g/g under optimized conditions. The water-absorption properties of starch-graft acrylic acid/zeolite/fly ash *via* the aqueous solution polymerization method was studied by Zhang *et al*. (2011). They found that the water absorption of the superabsorbent composite was 314.4 g/g. The present study gave a better result possibly because of the different zeolite and different method of modification used. The use of CTAB as an organic modifier was reported (Guo *et al*., 1999) to bring about tremendous increase in the dispersion capacity of zeolite.

Surface morphology of starch-g-poly (acrylic acid)/ organic-modified zeolite 4A superabsorbent composite

SEM images of starch-g-poly (acrylic acid), starch-g-poly (acrylic acid)/with 10 wt.% zeolite 4A, and starch-g-poly (acrylic acid)/organic-modified zeolite 4A with 10 wt.% superabsorbent composites are shown in Figure 8. The image of starch-g-poly (acrylic acid) (Figure 8a) shows a smooth and tight surface, but the addition of zeolite 4A leads to a rough surface (Figure 8b) which is convenient for the penetration of water into the polymeric network. Compared with starch-g-poly (acrylic acid) and starch-g-poly (acrylic acid)/zeolite 4A, starch-g-poly (acrylic acid)/organic-

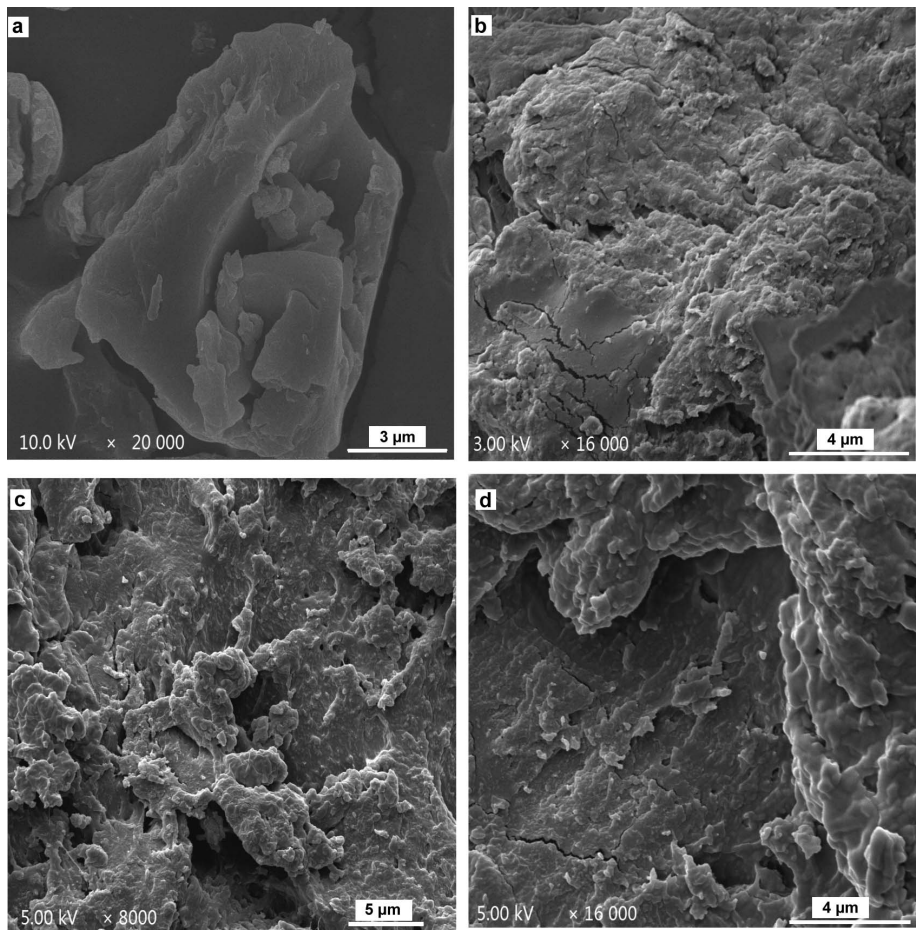

Figure 8. SEM images of (a) starch-g-poly (acrylic acid), (b) starch-g-poly (acrylic acid)/zeolite 4A without modification, (c, d) starch-g-poly (acrylic acid)/organic-modified zeolite 4A (zeolite 4A content = 10 wt.%; organic-modified 4A content under optimum modification conditions = 10 wt.%, potassium persulfate concentration = 5 g/L; MBA concentration = 5 g/L; reaction temperature = 70 ºC; reaction time = 3 h; neutralization degree = 80%).

https://doi.org/10.1346/CCMN.2014.0620305 Published online by Cambridge University Press

modified zeolite 4A superabsorbent composites (Figure 8c,d) has a coarse, polyporous, and corrugated surface. This surface structure also facilitates the permeation of water. Incorporation of zeolite 4A both with modification and without modification clearly introduces a rough surface which is related to equilibrium-water absorbency and swelling behaviors of the corresponding superabsorbent composites (Figure 8b–d). In addition, no phase separation is observed in Figure 8c or 8d. This morphology reconfirms the homogeneity of the superabsorbents synthesized as real superabsorbent composites.

Swelling kinetics analysis

The swelling kinetics in aqueous media for starch-g-poly (acrylic acid)/organic-modified zeolite 4A superabsorbent composite with 10 wt.% organic-modified zeolite 4A and starch-g-poly (acrylic acid) (Figure 9a) indicated that the profiles of swelling kinetics were similar. The degree of swelling increased quickly during the first 80 min after the immersion, reaching 95 wt.% of the equilibrium value in this time. The degree of swelling then increased slowly until the equilibrium was reached ~50 min later, depending on the products. Both have high initial swelling rates in distilled water. In general, the initial swelling rate is determined primarily by the penetration of water into the polymeric network through diffusion and capillarity (Mathakiya *et al.*, 1998). Osmotic pressure and chain relaxation may also be responsible for the high swelling rate.

The incorporation of organic-modified 4A zeolite within the starch-g-poly (acrylic acid) network increased the water-absorption capacity at equilibrium conditions. The water-absorption capacity of starch-g-poly (acrylic acid) composite is 320 g/g while that for starch-g-poly (acrylic acid)/organic-modified zeolite 4A superabsorbent composite is 410 g/g meaning that the introduction of organic-modified zeolite 4A into polymeric networks helps to improve the absorption capacity of superabsorbent composites. This behavior is because OH on the surface of organic-modified zeolite 4A increases the affinity of the polymeric network for water molecules. Another reason for the superabsorbent composite in traduced organic-modified zeolite 4A achieving greater absorption values may be that it has a coarse surface and capillarity is more evident, thereby accelerating the penetration of water molecules into the polymeric network.

Some of the characteristics collected from the swelling curves, used to evaluate the swelling mechan-

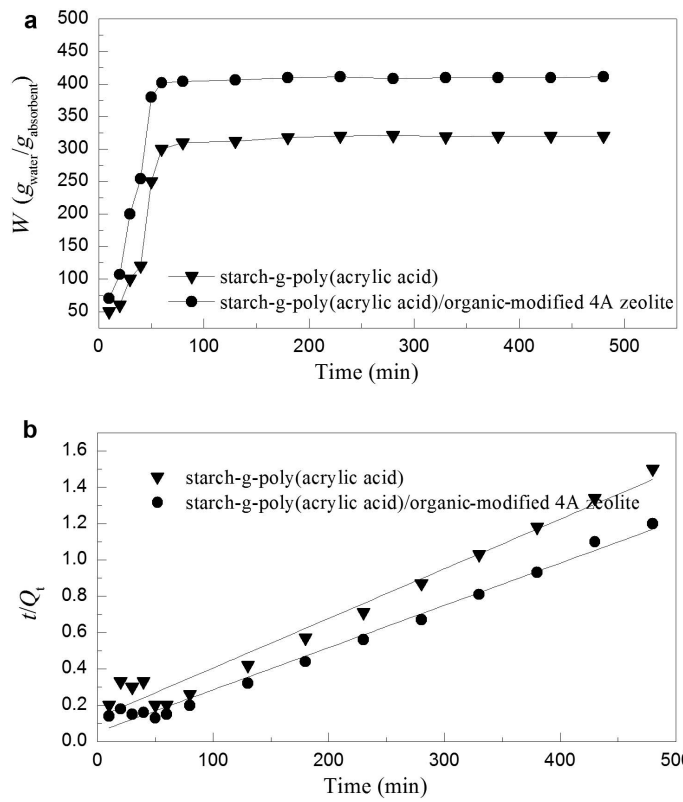

Figure 9. (a) Swelling kinetics curves and (b) t/Q_t *vs.* time plot for the starch-g-poly acrylic acid and starch-g-poly (acrylic acid)/organic-modified zeolite 4A superabsorbent composites (zeolite 4A content = 10 wt.%; organic-modified 4A content under optimum modification conditions = 10 wt.%; potassium persulfate concentration = 5 g/L; MBA concentration = 5 g/L; reaction temperature 70ºC; reaction time 3 h; neutralization degree = 80%).

https://doi.org/10.1346/CCMN.2014.0620305 Published online by Cambridge University Press

ism of superabsorbents – Schott's pseudo-second order swelling kinetics model (Schott, 1992) – were adopted to fit the experimental data. The pseudo-second order swelling kinetic model can be expressed through the relations proposed below:

$$t/Q_t = A + Bt \quad (6)$$

where: $$A = 1/kQ_\infty^2 \quad (7)$$

and $$B = 1/Q_\infty \quad (8)$$

where k is the constant rate for swelling, t is the swelling time, Q_t is a theoretical swelling value at moment t, and Q_∞ is a theoretical swelling value at equilibrium. Q_∞ and k were calculated by fitting experimental data (Figure 9a,b, equations 6–8).

Depending on experimental data, the plot of t/Q_t *vs.* the starch-g-poly(acrylic acid) and starch-g-poly(acrylic acid)/organic-modified 4A zeolite composite (Figure 9b) gave perfect straight lines with a good linear correlation coefficient ($R^2 > 0.98$), indicating that the swelling processes of the superabsorbents followed the Schott swelling kinetic model.

CONCLUSIONS

Organic-modified zeolite 4A particles as inorganic functional materials were first incorporated into the polymer with a view to manufacturing superabsorbent composites with good water-absorption properties. The zeolite Active index test, XRD, FTIR, and SEM were performed to evaluate the effects of surface treatment of zeolite 4A and RSM was used to investigate the optimum condition for the surface treatment. Starch-g-poly (acrylic acid) composites with doped organic-modified zeolite 4A were prepared by the aqueous-solution polymerization method and the water absorptions of the composites were determined. The experimental results indicated that CTAB has a significant effect on the surface modification of zeolite 4A. The water-absorption capacity increased with increasing organic-modified zeolite content up to 10 wt.%. At a 10 wt.% loading, the greatest capacity, 410 g/g, was reached. In addition, swelling-kinetics analysis in distilled water was performed and the results revealed that the introduction of the organic-modified zeolite 4A can improve the water-absorption capacity of the superabsorbent composite.

ACKNOWLEDGMENTS

The authors acknowledge the National Key Technology R&D Program of the Ministry of Science and Technology, P.R. China (No.2012BAC07B02) for support and for providing the funds to make this study possible.

REFERENCES

Ahmad, J. and Hägg, M. (2013) Preparation and characterization of polyvinyl acetate/zeolite 4A mixed matrix membrane for gas separation. *Journal of Membrane Science*, **427**, 73–84.

Alummoottil, N.J., Janardhanan, S., Subramoney, N.M., and Moothandaserry, S.S. (2010) Response surface methodology for the optimization and characterization of cassava starch-graft-poly (acrylamide). *Starch - Stärke*, **62**, 18–27.

Bernardi, A.C.D., Oliviera, P.P.A., Monte, M.B.D., and Barros, F.S. (2013) Brazilian sedimentary zeolite use in agriculture. *Microporous and Mesoporous Materials*, **167**, 16–21.

Bezerra, M.A., Santelli, R.E., Oliveira, E.P., Villar, L.S., and Escaleira, L.A. (2008) Response surface methodology (RSM) as a tool for optimization in analytical chemistry. *Talanta*, **76**, 965–977.

Dawood, A.S. and Li, Y. (2013) Modeling and optimization of new flocculant dosage and pH for flocculation: removal of pollutants from wastewater. *Water*, **5**, 342–355.

Faghihian, H., Moayed, M., Firooz, A., and Iravani, M. (2013) Synthesis, characterization, and evaluation of a ferromagnetically modified natural zeolite composite for removal of Cs^+ and Sr^{2+}. *Clays and Clay Minerals*, **61**, 193–203.

Ferreira, S.L.C., Bruns, R.E., Ferreira, H.S., Matos, G.D., David, J.M., Brandão, G.C., da Silva, E.G.P., Portugal, L.A., dos Reis, P.S., Souza, A.S., and Dos Santos, W.N.L. (2007) Box-Behnken design: An alternative for the optimization of analytical methods. *Analytica Chimica Acta*, **597**, 179–186.

Guo, L.P., Chen, Y.Z., and Yang, J. (1999) The surface modification of zeolite-4A by CTAB and its properties. *Journal of Wuhan University of Technology-Material*, **14**, 18–23.

Gworek, B. (1992) Inactivation of cadmium in contaminated soils using synthetic zeolites. *Environmental Pollution*, **75**, 269–271.

Haggerty, G.M. and Bowman, R.S. (1994) Sorption of chromate and other inorganic anions by organo-zeolite. *Environmental Science & Technology*, **28**, 452–458.

Hui, K.S., Chao, C.Y.H., and Kot, S.C. (2005) Removal of mixed heavy metal ions in wastewater by zeolite 4A and residual products from recycled coal fly ash. *Journal of Hazardous Materials*, **127**, 89–91.

Irani, M., Ismail, H., and Ahmad, Z. (2013) Preparation and properties of linear low-density polyethylene-g-poly (acrylic acid)/ organo-montmorillonite superabsorbent hydrogel composites. *Polymer Testing*, **32**, 502–512.

Khoonsap, S. and Amnuaypanich, S. (2011) Mixed matrix membranes prepared from poly(vinyl alcohol) (PVA) incorporated with zeolite 4A-graft-poly(2-hydroxyethyl methacrylate) (zeolite-g-PHEMA) for the pervaporation dehydration of water-acetone mixtures. *Journal of Membrane Science*, **367**, 182–189.

Lanthong, P., Nuisin R., and Kiatkamjornwong, S. (2006) Graft copolymerization, characterization, and degradation of cassava starch-g-acrylamide/itaconic acid superabsorbents. *Carbohydrate Polymers*, **66**, 229–245.

Le Van Mao, R., Sjiariel, B., and Dunnigan, J. (1991) Asbestos-derived zeolites as water-retaining materials in soils. *Zeolites*, **11**, 804–809.

Lee, W.F. and Yang, L.G. (2004) Superabsorbent polymeric materials. XII. Effect of montmorillonite on water absorbency for poly (sodium acrylate) and montmorillonite nanocomposite superabsorbents. *Journal of Applied Polymer Science*, **92**, 3422–3429.

Li, A. and Wang, A.Q. (2005) Synthesis and properties of clay-based superabsorbent composite. *European Polymer Journal*, **41**, 1630–1637.

Lokhande, H.T. and Gotmare, V.D. (1999) Utilization of textile loomwaste as a highly absorbent polymer through graft copolymerization. *Bioresource Technology*, **68**, 283–286.

Lundstedt, T., Seifert, E., Abramo, L., Thelin, B., Nyström, Å., Pettersen, J., and Bergman, R. (1998) Experimental design

and optimization. *Chemometrics and Intelligent Laboratory Systems*, **42**, 3–40.

Mathakiya, I., Vangani, V., and Rakshit, A.K. (1998) Terpolymerization ofacrylamide, acrylic acid, and acrylonitrile: Synthesis and properties. *Journal of Applied Polymer Science*, **69**, 217–228.

Misaelides, P. (2011) Application of natural zeolites in environmental remediation: A short review. *Microporous and Mesoporous Materials*, **144**, 15–18.

Mohana Raju, K. and Padmanabha Raju, M. (2001) Synthesis and swelling properties of superabsorbent copolymers. *Advances in Polymer Technology*, **20**, 146–154.

Razali, M.A., Sanusi, N., Ismail, H., Othman, N., and Ariffin, A. (2012) Application of response surface methodology (RSM) for optimization of cassava starch grafted polyDADMAC synthesis for cationic properties. *Starch - Stärke*, **64**, 935–943.

Rožić, M. and Miljanić, S. (2011) Sorption of HDTMA cations on Croatian natural mordenite tuff. *Journal of Hazardous Materials*, **185**, 423–429.

Saxena, S.K., Kumar, M., and Viswanadham, N. (2013) Studies on textural properties of lanthanum-exchanged Y zeolites as promising materials for value upgradation of Jatropha oil. *Journal of Materials Science*, **48**, 7949–7959.

Schott, H. (1992) Swelling kinetics of polymers. *Journal of Macromolecular Science Part B – Physics*, **31**, 1–9.

Spagnol, C., Rodrigues, F.H.A., Pereira, A.G.B., Fajardo, A.R., Rubira, A.F., and Muniz, E.C. (2012) Superabsorbent hydrogel nanocomposite based on starch-g-poly (sodium acrylate) matrix filled with cellulose nanowhiskers. *Cellulose*, **19**, 1225–1237.

Stojakovic, D., Milenkovic, J., Daneu, N., and Rajic, N. (2011) A study of the removal of copper ions from aqueous solution using clinoptilolite from Serbia. *Clays and Clay Minerals*, **59**, 277–285.

Wang, A. and Zhang, J.P. (2006) *High-Absorption Resin Composed of Organic and Inorganic Materials*. Science Press, Beijing.

Wang, C.Y., Zhou, J.T., He, J.K., Hao C.S., Pan Y.Z., and Meng, C.G. (2012) Synthesis of zeolite A and its application as a high-capacity cadmium ion exchanger. *Chinese Journal of Catalysis*, **33**, 1862–1869.

Wang, M.S., Liao, L.B., Zhang, X.L., Li, Z.H., Xia, Z.G., and Cao, W.D. (2011) Adsorption of low-concentration ammonium onto vermiculite from Hebei province, China. *Clays and Clay Minerals*, **59**, 459–465.

Wang, S.G., Gong, W.X., Liu, X.W., Gao, B.Y., Yue, Q.Y., and Zhang, D.H. (2006) Removal of fulvic acids from aqueous solutions via surfactant modified zeolite. *Chemical Research in Chinese Universities*, **22**, 566–570.

Weaver, M.O., Bagley, E.B., Fanta, G.F., and Doane, W.M. (1976) Highly absorbent starch-containing polymeric compositions. US Patent 3.981.100.

Zdanowicz, M., Schmidt, B., and Spychaj, T. (2010) Starch graft copolymers as superabsorbents obtained via reactive extrusion processing. *Polish Journal of Chemical Technology*, **12**, 14–17.

Zhang, J., Li, A., and Wang, A. (2006) Study on superabsorbent composite. VI. Preparation, characterization and swelling behaviors of starch phosphate-graft-acrylamide/attapulgite superabsorbent composite. *Carbohydrate Polymers*, **65**, 150–158.

Zhang, X.L., Li, Y.H., Hao, P.P., and Yang S. (2011) Research on synthesis and performance of water preserver starch-grafted acrylic acid/zeolite/fly ash. *Journal of Anhui Agricultural Science*, **39**, 3–5.

Zhou, B., Liao, R.K., Li, Y.K., Gu, T., Yang, P.L., Feng, J.,Xing, W.M., and Zou, Z.C. (2012) Water-absorption characteristics of organic–inorganic composite superabsorbent polymers and its effect on summer maize root growth. *Journal of Applied Polymer Science*, **126**, 423–435.

Zhou, J.P., Qiu, K.Q., and Fu, W.L. (2005) The surface modification of ZnO and its effect on the mechanical properties of filled polypropylene composites. *Journal of Composite Materials*, **39**, 1931–1941.

Zwingmann, N., Mackinnon, I.D.R., and Gilkes, R.J. (2011) Use of a zeolite synthesized from alkali treated kaolin as a K fertiliser: Glasshouse experiments on leaching and uptake of K by wheat plants in sandy soil. *Applied Clay Science*, **53**, 684–690.

(*Received 1 March 2014; revised 20 June 2014; AE: S.M. Kuznicki; Ms. 854*)